

# Bayesian Projection of Refugee and Asylum Seeker Populations

Herbert Susmann<sup>1</sup> and Adrian E. Raftery<sup>2</sup>

<sup>1</sup>Division of Biostatistics, Department of Population Health, NYU Grossman School of Medicine, USA. Email: susmah01@nyu.edu (Corresponding author)

<sup>2</sup>Departments of Statistics and Sociology, University of Washington, USA. Email: raftery@uw.edu

## Abstract

Estimates of future migration patterns are a crucial input to world population projections. Forced migration, including refugee and asylum seekers, plays an important role in overall migration patterns, but is notoriously difficult to forecast. We propose a modeling pipeline based on Bayesian hierarchical time-series modeling for projecting combined refugee and asylum seeker populations by country of origin using data from the United Nations High Commissioner for Human Rights (UNHCR). Our approach is based on a conceptual model of refugee crises following growth and decline phases, separated by a peak. The growth and decline phases are modeled by logistic growth and decline through an *interrupted logistic process model*. We evaluate our method through a set of validation exercises that show it has good performance for forecasts at 1, 5, and 10 year horizons, and we present projections for 35 countries with ongoing refugee crises.

**Keywords** Bayesian hierarchical model · Forced displacement · Population projections

## Introduction

World population projections are used for a number of reasons, including policy planning and as an input for projecting other outcomes of interest (Vanella et al., 2020). Population projections are formed based on projections of three basic demographic variables: births, deaths, and migration (Swanson et al., 2004). The third variable, migration, has traditionally been viewed as being harder to forecast than the first two due to inherent uncertainty in the political and economic factors that are drivers of migration (Fuchs et al., 2021; de Valk et al., 2022). Furthermore, forced displacement as a subset of international migration is particularly challenging to forecast because it can change rapidly; for example, the sudden outbreak of a war can lead very quickly to large numbers of refugees (Martin and Singh, 2018). Complicating matters further is that defining who qualifies as a forced migrant is in itself a complex political and legal subject (Reed et al., 2016).

The United Nations (UN) Population Division is a major producer of population projections through regular releases of the World Population Prospects, the most recent being from 2022 (United Nations, 2022b). The UN uses probabilistic Bayesian approaches for projecting total fertility and life expectancy (Alkema et al., 2011; Raftery et al., 2013). For forced migration, UN projections are currently based on an assumption that two thirds of refugees will return to their country of origin within 5 years (United Nations, 2022a). This paper is motivated by the goal of providing probabilistic projections of refugee and asylum seeker populations to serve as input for UN population projections.

Our forecasting approach is based on a conceptual model of refugee crises in which crises experience growth and decline phases, separated by a peak. The growth phase corresponds to refugees leaving their country of origin due to a conflict or other crisis. The peak is a period during which the refugees stay in their country of destination. During the decline stage, the refugees return home.

Trends on either side of the peak are modeled as following logistic growth (decline). We refer to this process model as an *interrupted logistic model*. We produce probabilistic projections using Bayesian statistical inference, drawing on the long lines of extant research applying Bayesian methods to estimate and project demographic indicators (Bijak, 2011; Bijak and Bryant, 2016; Raftery et al., 2014).

Other attempts have been made to apply statistical demography techniques to project forcibly displaced populations. Within the UN High Commissioner for Human Rights (UNHCR) there have been multiple efforts. The UNHCR Demographic Projection Tool applies demographic techniques to project age-specific refugee populations based on fertility and life expectancy data. However, the tool does not attempt to project arrivals or departures of refugees, rather relying on the analyst to provide possible future scenarios. From another angle, the UNHCR Jetson project seeks to apply predictive modeling to forecast refugee movements (UNHCR 2024a). A predictive model of monthly arrivals of internally displaced persons by region in Somalia was developed using climate, weather, and market variables as predictors (UNHCR 2024b).

Statistical and machine learning approaches have been used to predict refugee movements using indicators such as violent conflicts, market prices, and weather and climate variables (Carammia et al., 2022; Huynh and Basu, 2020; Singh et al., 2019). Typically, such methods have shorter forecast horizons (on the order of weeks or months) and are targeted towards aiding in humanitarian response efforts. Similarly, a number of countries have implemented prediction systems in order to anticipate arrivals of asylum seekers (Angenendt et al., 2023). Methods based on detecting signals in other variables are difficult to apply for long-term population projections, as doing so typically requires projecting the indicators themselves, which are often noisier than the demographic outcome being forecast. As such, our approach is based only on historical refugee and asylum seeker data. A possible downside of this approach is that our methods may be less well suited for short-term projections of the type useful for humanitarian planning in emergencies.

Gravity-type models have also been applied to predict forced migration flows (Qi and Bircan, 2023; Saldarriaga and Hua, 2019). However, the fundamental assumptions of gravity models have been criticized as insufficient in explaining human migration patterns (Beyer et al., 2022; Welch and Raftery, 2022). In addition, similar to the approaches described in the previous paragraph, gravity models typically depend on complex covariates including

economic, climate, and conflict variables. Projections based on gravity models therefore require projections of all covariates, which is difficult especially for long-term projections.

A related methodological area of research has been the development of agent-based models (ABMs) to simulate forced migration on a variety of geographic and temporal time scales (Gray et al., 2017; Sokolowski and Banks, 2014; Groen, 2016; Frydenlund et al., 2018; Kniveton et al., 2011). Typically ABMs simulate individual refugees according to a set of complex behavioral rules in order to form aggregate projections. However, the intensive computational requirements and unclear probabilistic properties of ABMs make them difficult to apply for longer-term forecasts, especially when statistically well-founded estimates of uncertainty are of interest.

The rest of the paper unfolds as follows. In the next section we describe the analysis dataset and propose the statistical methodology for our approach. Out-of-sample validations and substantive results are presented in the following section. We conclude with a discussion of the findings in the final section.

## Methods

### Data

In this paper, we focus on individuals classified as refugees or asylum seekers by UNHCR based on definitions in the International Recommendations on Refugee Statistics (EGRIS, 2018). The number of refugees by country of origin were sourced from the UNHCR Refugee Population Statistics Database (UNHCR, 2021). The UNHCR releases population statistics twice per year, with end of year statistics being released the following June. Based on definitions provided in the International Recommendations on Refugee Statistics, forcibly displaced and stateless populations are separated into five categories: refugees, asylum seekers, internally displaced persons of concern to UNHCR, other people in need of international protection, and stateless people (EGRIS, 2018). Statistics on each population type are available starting in different years depending on the host UN division.

Formally, let  $t = 1, \dots, T$  index years and  $c = 1, \dots, C$  index UN divisions (henceforth referred to generically as “countries”). The UN divisions “Unknown”, “Stateless”, “Western Sahara”, and “Palestinian” were excluded from the analysis – Western Sahara for data quality concerns (U.S. Department of State 2007), and Palestinian because those data are sourced differently than other divisions (UNHCR, 2021). Let  $R_{c,t}$  be the combined number of refugees and asylum seekers with origin country  $c$  at time  $t$ . Let  $P_{c,t}$  be the population of country  $c$  at time  $t$ , using as source the UN World Population Prospects 2022 (United Nations, 2022b). We model refugee populations as proportions, defining  $r_{c,t} = R_{c,t} / (R_{c,t} + P_{c,t})$ . The analysis dataset was formed by selecting countries with at least 10 years of observed data, at least one observed refugee proportion  $r_{c,t}$  greater than 1%, and at least one observed total number of refugees  $R_{c,t}$  greater than 1000.

### Conceptual Framework

We conceptualize the number of refugees and asylum seekers from a particular country over time as arising from a succession of one or more crises, which we refer to generically as a

*refugee crisis* although it may lead to both refugees and asylum seekers. We think of a refugee crisis as being caused by ongoing events or conditions in the country, such as war, famine, or political/economic upheaval. The refugee and asylum seeker population is expected to increase while the condition is present, before declining after the condition ends. A refugee crisis thus comprises two stages: an initial growth stage and a decline phase, separated by a peak.

Figure 1 shows illustrative data from three countries. In Mozambique, a driver of the refugee population was the Mozambican Civil War from 1977-1992. Thus, we see a sharp increase in the refugee population during the war, a peak in 1992 when the war ended, followed by a decline. Somalia appears to have experienced two crises, with the most recent crisis currently in the decline phase. Honduras appears to currently be in the growth phase of a crisis, and the timing and magnitude of the peak of the crisis is not yet known.

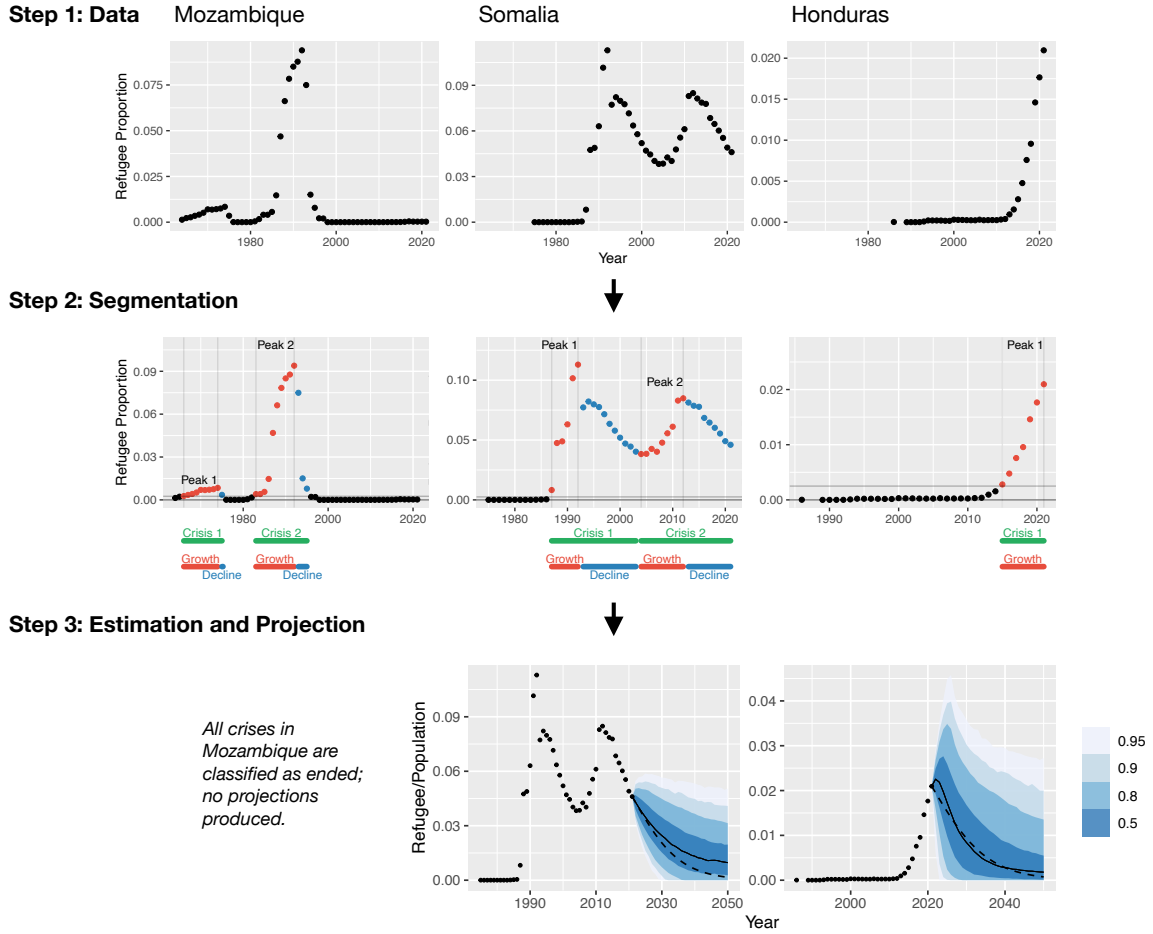


Figure 1: Overall modeling pipeline for projecting refugee and asylum seeker populations. Step 1 illustrates the observed data from Mozambique, Somalia, and Honduras. In Step 2, the data are segmented into multiple refugee crises. In Step 3, projections are produced for ongoing crises.

## Modeling Approach

Our modeling approach is informed by the conceptual framework for refugee crises. First, refugee and asylum seeker populations from each origin country are divided into segments corresponding to refugee crises. Next, a Bayesian hierarchical model of refugee crises is fit based on the segmented dataset. The overall pipeline is illustrated in Figure 1 using Mozambique, Somalia, and Honduras as examples.

**Segmentation** The time series for each country are first segmented into one or more refugee crises. We do so by identifying local peaks in the time series, which we take to be the peak of a corresponding refugee crisis. To identify local peaks we use a peak detection algorithm described by Palshikar et al. (2009) and implemented in the `scorepeak` package (Ochi, 2019). Once the peaks are identified, we identify the extent of the refugee crisis by looking for troughs before and after the peak. A *trough* is defined as the minimum proportion observed between two peaks (or between a peak and the beginning or end of the time series). The start of a crisis is defined as the first year after a trough (or the beginning of the time-series) in which the refugee proportion  $r_{c,t}$  is greater than 0.025%. If such a year does not exist, the start is considered to be the year before the peak.

Each crisis is next classified as ended or ongoing. A crisis is classified as ended if it is either followed by another crisis, or if the most recent observed refugee proportion  $r_{c,t}$  is less than 0.025%. For an ended crisis, the end time point is set to the year in which the last observation was greater than 0.025%. All other crises are classified as ongoing. Ongoing crisis are further divided into being in the growth or decline phase. Countries that have a detected local peak on or after 2015, or that have a refugee proportion in 2021 greater than 80% of the most recent peak, are classified as being in the growth phase. All other ongoing crises are classified as being in the decline phase.

Figure 1 illustrates the detected crises for Mozambique, Somalia, and Honduras. Two crises are detected in Mozambique, corresponding roughly to the Mozambican War of Independence and the Mozambican Civil War. The second crisis in Mozambique is classified as having ended, as all observations after 1995 are under 0.025%. Somalia also has two crises detected, corresponding to different phases of the Somali Civil War. The second crisis in Somalia is classified as ongoing and in the decline phase, as the most recent observations are all over 0.025%. Finally, an ongoing crisis is also detected in Honduras, but is classified as being in the growth phase. Table 1 shows the classifications of the final crisis in each country in the analysis dataset.

Formally, let  $m = 1, \dots, M$  index the detected refugee crises from the segmentation step, and denote by  $c[m]$  the country corresponding to the  $m$ th crisis. Let  $t_m^{\text{start}}, t_m^{\text{end}}$  be the start and end time points of the  $m$ th crisis, respectively. Let  $t_m^{\text{peak}}$  be the time point of the peak of crisis  $m$ .

**Process Model** Let  $\mu_{c,t}$  denote the modeled refugee proportion in country  $c$  at time  $t$ . The process model describes how  $\mu_{c,t}$  is expected to evolve over time (Susmann et al., 2022). The core of our modeling approach is to assume that refugee populations follow logistic growth and decline trends during the growth and decline phases of a refugee crisis, respectively. The rate of change of  $\mu_{c[m],t}$  during the growth and decline phases is modeled by the following

Table 1: Countries in the analysis dataset grouped by classification of their most recent crisis.

<p><b>Ended crises</b>  Angola, Cambodia, Chad, Equatorial Guinea, Ethiopia, Guinea-Bissau, Lao People’s Dem. Rep., Liberia, Mozambique, Namibia, Sierra Leone, Slovenia, Tajikistan, Timor-Leste, Togo, Uganda, Zimbabwe</p>
<p><b>Ongoing crises, decline phase</b>  Afghanistan, Azerbaijan, Bhutan, Burundi, Colombia, Croatia, Gambia, Rwanda, Serbia and Kosovo: S/RES/1244 (1999), Somalia</p>
<p><b>Ongoing crises, growth phase</b>  Albania, Armenia, Bosnia and Herzegovina, Central African Rep., Congo, Dem. Rep. of the Congo, Djibouti, El Salvador, Eritrea, Georgia, Guatemala, Guinea, Guinea-Bissau, Haiti, Honduras, Iraq, Lebanon, Mali, Mauritania, Myanmar, Nicaragua, South Sudan, Sri Lanka, Sudan, Syrian Arab Rep., Venezuela (Bolivarian Republic of)</p>

logistic rate function:

$$f(\mu_{c[m],t}, \omega, \lambda) = \begin{cases} \lambda - \mu_{c[m],t}, & \mu_{c[m],t} > \lambda, \\ \omega \cdot \mu_{c[m],t} \left(1 - \frac{\mu_{c[m],t}}{\lambda}\right), & \text{otherwise.} \end{cases}$$

where  $\omega \in \mathbb{R}$  is a rate parameter and  $\lambda \in (0, 1)$  is an asymptote parameter. During the growth phase, a crisis-specific rate parameter  $\omega_m^{(1)} > 0$  is applied. During the decline phase a rate parameter  $\omega_m^{(2)} < 0$  is used. Both growth and decline phases share an asymptote parameter  $\lambda_m$ . Formally, the expected rate of change for crisis  $m$  at time  $t$  is given by

$$\xi_{m,t} = \begin{cases} f(r_{c[m],t-1}, \omega_m^{(1)}, \lambda_m), & t_m^{\text{start}} \leq t \leq t_m^{\text{peak}}, \\ f(r_{c[m],t-1}, \omega_m^{(2)}, \lambda_m), & t_m^{\text{peak}} < t \leq t_m^{\text{end}}. \end{cases}$$

We refer to the process model as an *interrupted logistic process model* because the logistic growth during the growth phase is interrupted at time  $t_m^{\text{peak}}$ . Figure 2 illustrates the parameters of the interrupted logistic model for a single crisis.

**Data Model** We assume that the observed rate of change is normally distributed around the expected rate of change, with country-specific variance terms that differ for the growth and decline phases:

$$r_{c[m],t} - r_{c[m],t-1} \sim N(\xi_{m,t}, \sigma_{c,t}^2),$$

where

$$\sigma_{c,t} = \begin{cases} \sigma_c^{(1)}, & t \leq t_m^{\text{peak}}, \\ \sigma_c^{(2)}, & t > t_m^{\text{peak}}. \end{cases}$$

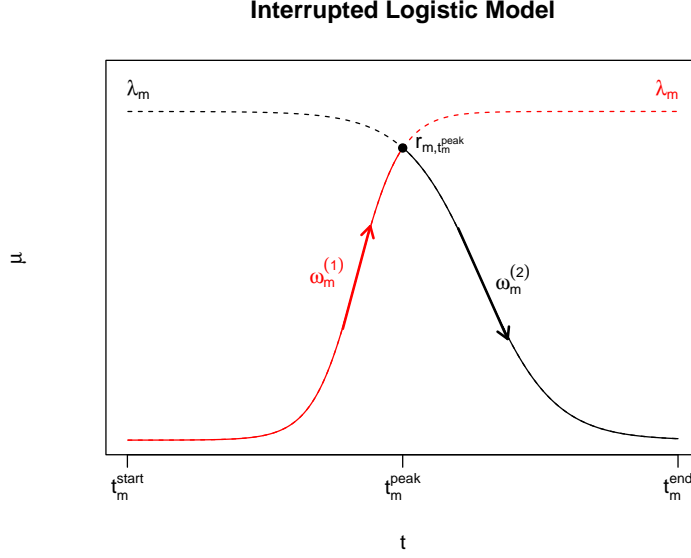


Figure 2: Diagram of the interrupted logistic process model.

**Crisis lengths and maxima** We model the length of the growth phase and the refugee proportion observed at the peak for use in projecting crises that are still in the growth phase. The length of the growth phase is assumed to be exponentially distributed with rate parameter  $\psi > 0$ :

$$t_m^{\text{peak}} - t_m^{\text{start}} \sim \text{Exp}(\psi).$$

The exponential model was chosen based on empirical inspection of the distribution of growth phase lengths (Appendix Figure 6). The proportion at the peak is assumed to follow a logit-normal distribution around a mean parameter  $\rho$ :

$$\text{logit}(r_{c[m], t_m^{\text{peak}}}) \sim N(\rho, \sigma_\rho^2),$$

where  $\text{logit}(x) = \log(x/(1-x))$ .

**Hierarchical Priors** Hierarchical priors are used to share information between crises. The upper asymptote of each crisis is assumed to follow a logit-normal distribution around an overall mean:

$$\text{logit}(\lambda_m) \sim N(\lambda_g, \sigma_\lambda^2).$$

The growth and decline rate are assumed to follow a Student's  $t$ -distribution around an overall mean:

$$\begin{aligned} \omega_m^{(1)} &\sim t_3(\mu_{\omega^{(1)}}, \sigma_{\omega^{(1)}}^2), \\ \omega_m^{(2)} &\sim t_3(\mu_{\omega^{(2)}}, \sigma_{\omega^{(2)}}^2). \end{aligned}$$

where  $t_\nu(\mu, \sigma^2)$  denotes a non-centered Student's  $t$ -distribution with  $\nu$  degrees of freedom, location  $\mu$  and scale  $\sigma^2$ . The Student's  $t$ -distribution was chosen to allow for outlier growth and decline rates. Similar hierarchical priors are used for the growth and decline noise parameters:

$$\begin{aligned}\sigma_c^{(1)} &\sim N(\mu_{\sigma^{(1)}}, \sigma_{\sigma^{(1)}}^2), \\ \sigma_c^{(2)} &\sim N(\mu_{\sigma^{(2)}}, \sigma_{\sigma^{(2)}}^2).\end{aligned}$$

## Projections

Projections are produced for all ongoing crises. Suppose we have at our disposal  $k = 1, \dots, K$  posterior draws from the joint posterior distribution of the model parameters conditional on all the observed data. We will write  $\alpha^{(k)}$  to denote the  $k$ th posterior draw of a parameter  $\alpha$ .

The projection method is different depending on whether the ongoing crisis was classified as being in the decline or growth phase. For a crisis  $m$  that is ongoing and in the decline phase, the timing and level of the peak is taken as fixed. Thus, for all  $t > t_m^{\text{last}}$ , the refugee proportion is projected by recursive application of the following equation for each posterior draw  $k = 1, \dots, K$ :

$$\mu_{c[m],t}^{(k)} \sim N\left(\mu_{c[m],t-1}^{(k)} + f\left(\mu_{c[m],t-1}^{(k)}, \omega_m^{(2)(k)}, \lambda_m^{(k)}\right), \left(\sigma_{c,t}^{(k)}\right)^2\right),$$

and where we set the initial value  $\mu_{c[m],t_m^{\text{last}}}^{(k)} = r_{c[m],t_m^{\text{last}}}$ . If, for any time  $t$ ,  $\mu_{c[m],t}^{(k)} < 0$ , then we set  $\mu_{c[m],t}^{(k)} = 0.001$  before continuing recursive application of the formula.

For an ongoing crisis  $m$  in the growth phase, the timing and level of the peak has not been observed, and we integrate over this uncertainty. Suppose the peak falls in year  $t_m^{\text{last}} + \delta$ , where  $\delta \in \mathbb{N}^+$  (in practice we take  $\delta \in \{0, 1, \dots, 15\}$ ). Conditional on  $\delta$ , projections are generated by recursive application of the equation

$$\mu_{c[m],t+\delta}^{(k)} \sim \begin{cases} N\left(\mu_{c[m],t,\delta}^{(k)} + f\left(\mu_{c[m],t,\delta}^{(k)}, \omega_m^{(1)(k)}\right), \lambda_m^{(k)}, (\sigma_{c,t}^{(k)})^2\right), & t \leq t_m^{\text{last}} + \delta, \\ N\left(\mu_{c[m],t,\delta}^{(k)} + f\left(\mu_{c[m],t,\delta}^{(k)}, \omega_m^{(2)(k)}\right), \lambda_m^{(k)}, (\sigma_{c,t}^{(k)})^2\right), & t > t_m^{\text{last}} + \delta. \end{cases}$$

As before, if for any  $t$   $\mu_{c[m],t,\delta}^{(k)} < 0$ , then we set  $\mu_{c[m],t,\delta}^{(k)} = 0.001$ . Next, the probability of  $\delta$  conditional on the implied crisis length and the refugee proportion at the peak is calculated conditional on the crisis length parameters  $\psi$  and peak proportion parameters  $\rho$  and  $\sigma_\rho^2$  previously estimated.

$$p_\delta \propto d_{\text{Exp}}(\delta \mid \psi^{(k)}) d_N(\text{logit}(\mu_{c[m],t_m^{\text{last}}+\delta,\delta}^{(k)}) \mid \rho, \sigma_\rho^2),$$

where  $d_{\text{Exp}}$  is the density of the Exponential distribution and  $d_N$  the density of the normal distribution. A final peak position  $\delta^*$  is drawn with probabilities  $p_\delta$ , and the final projections are set to  $\mu_{c[m],t}^{(k)} = \mu_{c[m],t,\delta^*}^{(k)}$ . Figure 3 illustrates how projections for ongoing growth crises are generated conditional on  $\delta$ .



### Interrupted Logistic Model: Unknown Peak

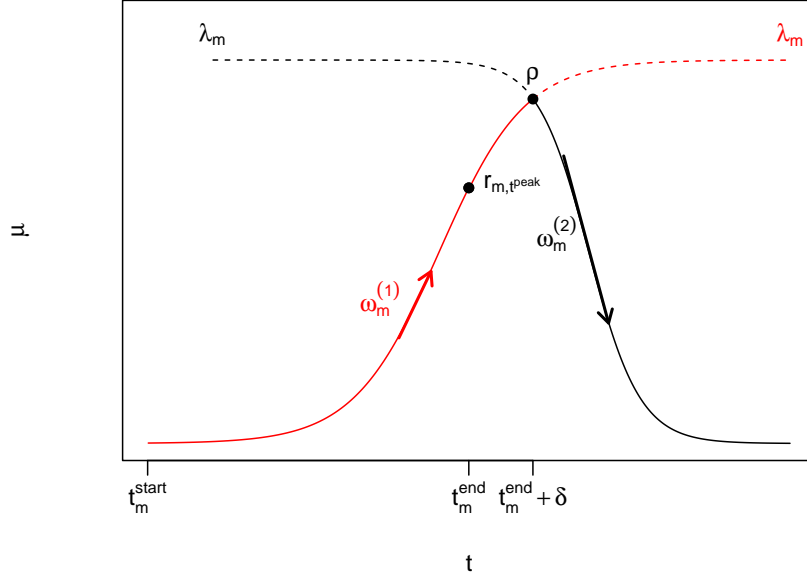


Figure 3: Diagram of projections for ongoing crisis in the growth phase. Projections are generated conditional on a parameter  $\delta$  that controls how long the crisis will continue before reaching its peak.

### Benchmark

As a benchmark we implemented a deterministic projection method based on the United Nations current rule of thumb that assumes two thirds of refugees will return to their country of origin within 5 years (United Nations, 2022a). We assume that the last observed value is at the midpoint of a logistic decline curve. Taken together, these assumptions imply a logistic rate of change of

$$\omega^* = -\frac{1}{5} \log 2.$$

Projections for any year  $t$  in a country  $c$  with final observed value at  $t_c^{\text{last}}$  are then given by

$$\mu_{c,t}^* = \frac{2r_{c,t_c^{\text{last}}}}{1 + \exp(\omega^*(t - t_c^{\text{last}}))}.$$

## Results

### Validation

As a validation exercise, we held out all observations after a cutoff time point  $t^*$  and applied the full projection pipeline. The validation set included all countries that did not have a new crisis start after the cutoff time point.

Table 2: Mean Absolute Error (MAE) and Mean Error (ME) of posterior median projections in the validation exercises.

Cutoff	Target	$n$	MAE		ME	
			Bayes	Logistic	Bayes	Logistic
<i>1 year ahead</i>						
2016	2017	25	<b>0.73</b>	0.82	<b>0.62</b>	0.75
2017	2018	26	<b>0.20</b>	0.28	<b>0.05</b>	0.23
2018	2019	26	<b>0.13</b>	0.20	<b>-0.03</b>	0.18
2019	2020	28	<b>0.15</b>	0.27	<b>0.01</b>	0.22
2020	2021	29	<b>0.26</b>	0.43	<b>0.20</b>	0.40
<i>5 year ahead</i>						
2011	2016	16	<b>1.46</b>	1.58	0.89	<b>0.79</b>
2016	2021	22	1.85	<b>1.76</b>	<b>1.67</b>	1.70
<i>10 year ahead</i>						
2011	2021	13	<b>2.26</b>	2.28	1.88	<b>1.77</b>

The mean error and mean absolute error for the proposed Bayesian method and the benchmark deterministic logistic method were computed for 1-year, 5-year, and 10-year projection horizons. The results are presented in Table 2. For the 1-year ahead projections, the Bayesian method had lower mean error and mean absolute error than the benchmark. The benchmark performed slightly better in terms of mean error for the 5- and 10-year projections than the Bayesian method.

For the Bayesian method we computed the 80%, 90%, and 95% empirical coverage rates of the corresponding credible intervals. The results are shown in Table 3. The small sizes of the validation sets make it difficult to draw strong conclusions as to the quality of the model calibration. For the 1-year ahead projections, the credible intervals are generally conservative, with the 80% intervals tending to have higher than nominal empirical coverage. The longer-term projections exhibit reasonable performance, with for example the 5-year ahead projections from 2016 having near-nominal 77.3%, 86.4%, and 95.5% empirical coverage for the 80%, 90%, and 95% credible intervals, respectively.

## Projections

Projections for all countries with an ongoing crisis detected as of 2021 are included in the appendix. Illustrative projections for six of these countries are shown in Figure 4. Of these countries, Colombia, Gambia, and Somalia have crises in the decline phase, and El Salvador, Haiti, and Honduras have crisis in the growth phase. The strength of the probabilistic projections from the Bayesian model as compared to the deterministic benchmark can be seen in Honduras. Despite the posterior median projection being similar to the deterministic projection, the Bayesian credible intervals indicate the possibility of continued growth in the refugee and asylum seeker population. In Gambia, the posterior median projects faster decline than the deterministic benchmark because the Bayesian model incorporates the previous rates of decline observed in the crisis.

Figure 5 illustrates how projections for El Salvador would have changed year over year as

Table 3: Empirical coverage of 80%, 90%, and 95% credible intervals for projections in the validation exercises.

Cutoff	Target	$n$	Coverage		
			80%	90%	95%
<i>1 year ahead</i>					
2016	2017	25	88.0%	88.0%	88.0%
2017	2018	26	100.0%	100.0%	100.0%
2018	2019	26	96.2%	100.0%	100.0%
2019	2020	28	96.4%	96.4%	96.4%
2020	2021	29	89.7%	89.7%	93.1%
<i>Average</i>			94.0%	94.8%	95.5%
<i>5 year ahead</i>					
2011	2016	16	75.0%	81.2%	87.5%
2016	2021	22	81.8%	86.4%	100.0%
<i>10 year ahead</i>					
2011	2021	13	76.9%	84.6%	84.6%

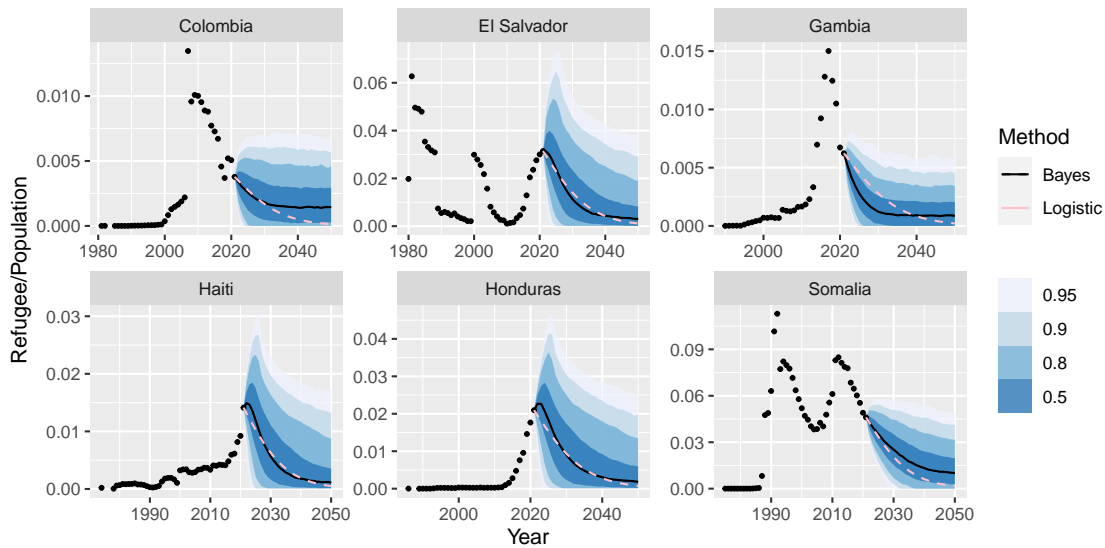


Figure 4: Projections for six illustrative countries. Shaded bands show the 50%, 80%, 90%, and 95% credible intervals. The pink dotted line shows the benchmark deterministic projection method.

new data became available. In 2016, the 95% credible intervals include the possibility of an increase in the refugee population to around the same level as the peak of the previous crisis. For the 2017 estimates, the model adjusts upwards its projections based on the increased rate of change implied by the new data point. By 2021, the posterior median suggests the crisis has reached its peak, although there is still significant posterior mass on the possibility of continued increases up a level last seen in the first refugee crisis in the country in the 1980s.

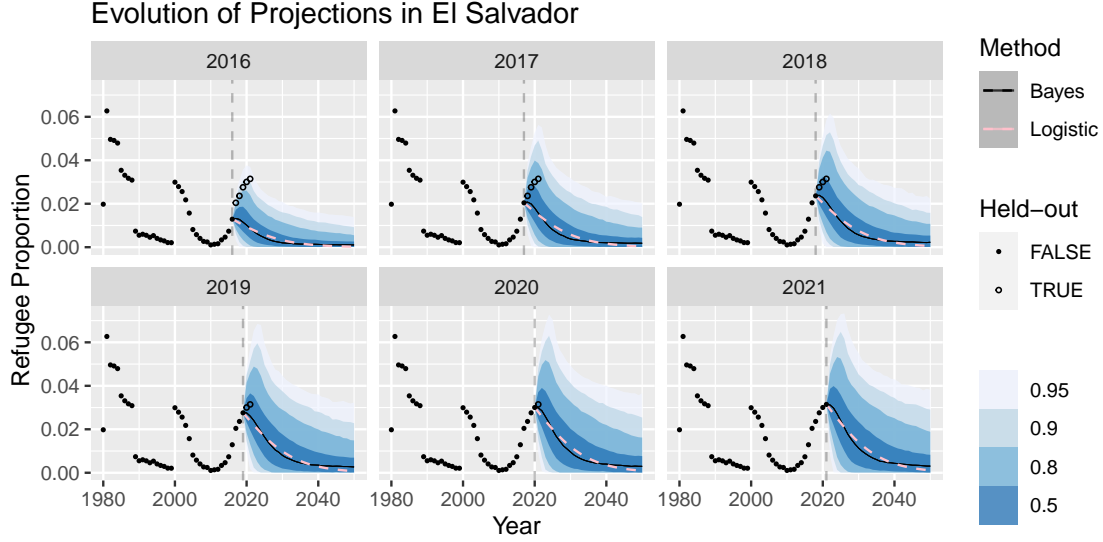


Figure 5: Projections in El Salvador from 2016-2021. Shaded bands show the 50%, 80%, 90%, and 95% credible intervals, respectively. The pink dotted line shows the benchmark deterministic projection method.

## Discussion

We have proposed a Bayesian hierarchical time-series model of refugee and asylum seeker populations by country of origin. We then used the model to project future combined refugee and asylum seeker populations for countries experiencing ongoing refugee crises. Validation exercises suggest the model is well-calibrated at multiple time horizons.

Current UN population projections assume that two thirds of refugees will return to their country of origin within 5 years (United Nations, 2022a). Our validation results show that this rule of thumb performs well for 5-year ahead projections. The Bayesian modeling approach achieves comparable or better performance in all the validation exercises, and has the additional benefit of providing well-calibrated probabilistic projections.

A basic assumption of any statistical forecasting method is that the future will be in some way similar to the past. In this work, this assumption manifests itself in the model specification that assumes current refugee crises will follow a similar shape to previous crises. However, the underlying dynamics of forced displacement may change in the future in ways that fundamentally change refugee population trends. Global climate change is a prominent example of a factor that may drive future displacement in ways that differ from past causes of displacement (Piguet et al., 2011). Uncertainty estimates from our modeling approach, however, are conditional on the model specification and do not incorporate uncertainty in how displacement dynamics may change in the future. As such, while credible intervals from our approach appear to be relatively well-calibrated in the projection horizons considered in the validation exercises, there is no guarantee that the model specification will lead to good performance in the long term.

Our work leaves open multiple directions for future research. We did not attempt to forecast the outbreak of new crises, rather focusing on projecting the end of already existing

crises. This focus encodes an optimistic assumption that, in the long term, all refugee crises will end. However, research has been carried out on identifying where and when future refugee crises will occur (OECD, 2019). Producing accurate “early warnings” of crises is notoriously difficult due to the complexity of causes of refugee crises (Schmeidl and Jenkins, 1996). An area for future research is to expand our approach to incorporate uncertainty about whether new crises will arise in the future. In addition, incorporating estimates of refugee and asylum seeker populations in country-level population projections requires projecting destination countries. We plan to address this in the future, drawing on developments in projecting bilateral migration flows between countries (Welch and Raftery, 2022).

**Acknowledgements:** This research was supported by NIH grant R01 HD070936. The authors thank Patrick Gerland for helpful conversations.

## References

- Alkema, L., Raftery, A. E., Gerland, P., Clark, S. J., Pelletier, F., Buettner, T., and Heilig, G. K. (2011). Probabilistic Projections of the Total Fertility Rate for All Countries. *Demography*, 48(3):815–839.
- Angenendt, S., Koch, A., and Tjaden, J. (2023). Predicting irregular migration: High hopes, meagre results.
- Beyer, R. M., Schewe, J., and Lotze-Campen, H. (2022). Gravity models do not explain, and cannot predict, international migration dynamics. *Humanities and Social Sciences Communications*, 9(1):56.
- Bijak, J. (2011). *Forecasting international migration in Europe: a Bayesian view*. The Springer series on demographic methods and population analysis. Springer, Dordrecht.
- Bijak, J. and Bryant, J. (2016). Bayesian demography 250 years after Bayes. *Population Studies*, 70(1):1–19. PMID: 26902889.
- Carammia, M., Iacus, S. M., and Wilkin, T. (2022). Forecasting asylum-related migration flows with machine learning and data at scale. *Scientific Reports*, 12(1):1457.
- de Valk, H. A. G., Acostamadiedo, E., Guan, Q., Melde, S., Mooyaart, J., Sohst, R. R., and Tjaden, J. (2022). *How to Predict Future Migration: Different Methods Explained and Compared*, pages 463–482. Springer International Publishing, Cham.
- EGRIS: Expert Group on Refugee and Internally Displaced Persons Statistics (2018). *International recommendations on refugee statistics*. Publications Office of the European Union.
- Frydenlund, E., Foytik, P., Padilla, J. J., and Ouattara, A. (2018). Where are they headed next? modeling emergent displaced camps in the DRC using agent-based models. In *Proceedings of the 2018 Winter Simulation Conference, WSC ’18*, page 22–32. IEEE Press.

- Fuchs, J., Söhnlein, D., and Vanella, P. (2021). Migration forecasting—significance and approaches. *Encyclopedia*, 1(3):689–709.
- Gray, J., Hilton, J., and Bijak, J. (2017). Choosing the choice: Reflections on modelling decisions and behaviour in demographic agent-based models. *Population Studies*, 71(sup1):85–97.
- Groen, D. (2016). Simulating refugee movements: Where would you go? *Procedia Computer Science*, 80:2251–2255. International Conference on Computational Science 2016, ICCS 2016, 6-8 June 2016, San Diego, California, USA.
- Huynh, B. Q. and Basu, S. (2020). Forecasting internally displaced population migration patterns in Syria and Yemen. *Disaster Medicine and Public Health Preparedness*, 14(3):302–307.
- Kniveton, D., Smith, C., and Wood, S. (2011). Agent-based model simulations of future changes in migration flows for Burkina Faso. *Global Environmental Change*, 21:S34–S40. Migration and Global Environmental Change – Review of Drivers of Migration.
- Martin, S. F. and Singh, L. (2018). Data Analytics and Displacement: Using Big Data to Forecast Mass Movements of People. In *Digital Lifeline?: ICTs for Refugees and Displaced Persons*. The MIT Press.
- Ochi, S. (2019). *scorepeak: Peak Functions for Peak Detection in Univariate Time Series*. R package version 0.1.2.
- OECD (2019). Anticipating, monitoring and reacting to inflows of refugees and other vulnerable migrants. In *Ready to Help?: Improving Resilience of Integration Systems for Refugees and other Vulnerable Migrants*. OECD Publishing, Paris.
- Palshikar, G. et al. (2009). Simple algorithms for peak detection in time-series. In *Proc. 1st Int. Conf. Advanced Data Analysis, Business Analytics and Intelligence*, volume 122.
- Piguat, E., Pécoud, A., and de Guchteneire, P. (2011). Migration and climate change: An overview. *Refugee Survey Quarterly*, 30(3):1–23.
- Qi, H. and Bircan, T. (2023). Modelling and predicting forced migration. *PLOS ONE*, 18(4):1–21.
- Raftery, A. E., Alkema, L., and Gerland, P. (2014). Bayesian population projections for the United Nations. *Statistical Science*, 29(1):58 – 68.
- Raftery, A. E., Chunn, J. L., Gerland, P., and Ševčíková, H. (2013). Bayesian Probabilistic Projections of Life Expectancy for All Countries. *Demography*, 50(3):777–801.
- Reed, H. E., Ludwig, B., and Braslow, L. (2016). Forced migration. In White, M. J., editor, *International Handbook of Migration and Population Distribution*, pages 605–625. Springer Netherlands, Dordrecht.

- Saldarriaga, J. F. and Hua, Y. (2019). A gravity model analysis of forced displacement in Colombia. *Cities*, 95:102407.
- Schmeidl, S. and Jenkins, J. C. (1996). Issues in quantitative modelling in the early warning of refugee migration. *Refuge: Canada's Journal on Refugees / Refuge: Revue canadienne sur les réfugiés*, 15(4):4–7.
- Singh, L., Wahedi, L., Wang, Y., Wei, Y., Kirov, C., Martin, S., Donato, K., Liu, Y., and Kawintiranon, K. (2019). Blending noisy social media signals with traditional movement variables to predict forced migration. In *Proceedings of the 25th ACM SIGKDD International Conference on Knowledge Discovery & Data Mining*, KDD '19, page 1975–1983, New York, NY, USA. Association for Computing Machinery.
- Sokolowski, J. A. and Banks, C. M. (2014). A methodology for environment and agent development to model population displacement. In *Proceedings of the 2014 Symposium on Agent Directed Simulation*, ADS '14, San Diego, CA, USA. Society for Computer Simulation International.
- Susmann, H., Alexander, M., and Alkema, L. (2022). Temporal models for demographic and global health outcomes in multiple populations: Introducing a new framework to review and standardise documentation of model assumptions and facilitate model comparison. *International Statistical Review*, 90(3):437–467.
- Swanson, D. A., Siegel, J. S., and Shryock, H. S. (2004). *The Methods and materials of demography*. Elsevier Academic Press, San Diego, CA, second edition.
- UNHCR (2021). UNHCR refugee population statistics database. <https://www.unhcr.org/refugee-statistics>.
- UNHCR Innovation Service. Jetson technical specifications. <https://jetson.unhcr.org/tech.html>. Accessed: 2024-02-27.
- UNHCR Innovation Service. Project jetson. <https://jetson.unhcr.org/index.html>. Accessed: 2024-02-27.
- United Nations, Department of Economic and Social Affairs, Population Division (2022a). World population prospects 2022: Methodology of the United Nations population estimates and projections. Technical Report UN DESA/POP/2022/TR/NO. 4.
- United Nations, Department of Economic and Social Affairs, Population Division (2022b). World population prospects 2022, online edition.
- U.S. Department of State, Bureau of Democracy, Human Rights, and Labor (2007). Western sahara, country reports on human rights practices. <https://2001-2009.state.gov/g/drl/rls/hrrpt/2007/102555.htm>. [Online; accessed 9-May-2024].
- Vanella, P., Deschermeier, P., and Wilke, C. B. (2020). An overview of population projections—methodological concepts, international data availability, and use cases. *Forecasting*, 2(3):346–363.

Welch, N. G. and Raftery, A. E. (2022). Probabilistic forecasts of international bilateral migration flows. *Proceedings of the National Academy of Sciences*, 119(35):e2203822119.



## Appendix

### Hyperpriors

Peak values:

$$\begin{aligned}\rho &\sim N(0, 3), \\ \sigma_\rho &\sim \text{InvGamma}(0.1, 0.1).\end{aligned}$$

Peak duration:

$$\psi \sim \text{InvGamma}(0.1, 0.1).$$

Growth and decline rates:

$$\begin{aligned}\mu_{\omega^{(1)}} &\sim N(0, 3), \\ \mu_{\omega^{(2)}} &\sim N(0, 3), \\ \sigma_{\omega^{(1)}} &\sim \text{InvGamma}(0.1, 0.1), \\ \sigma_{\omega^{(2)}} &\sim \text{InvGamma}(0.1, 0.1).\end{aligned}$$

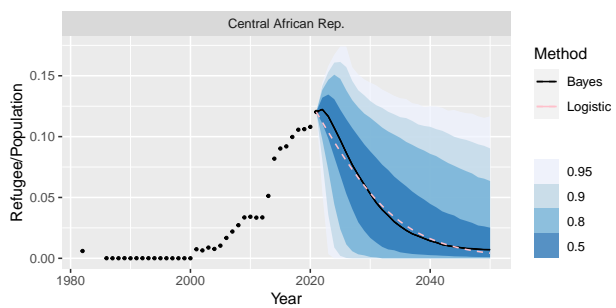
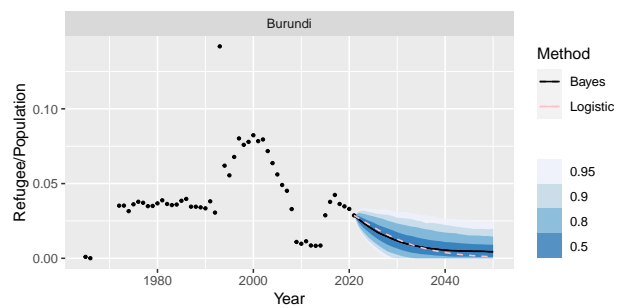
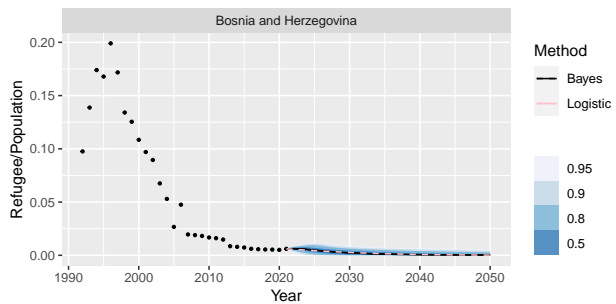
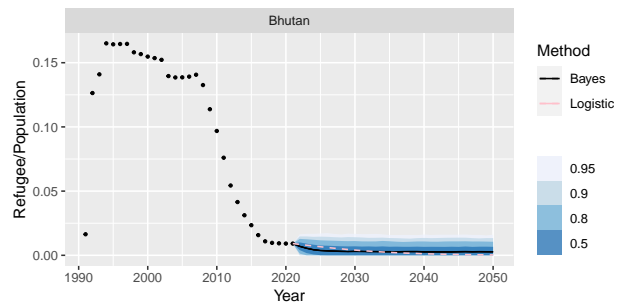
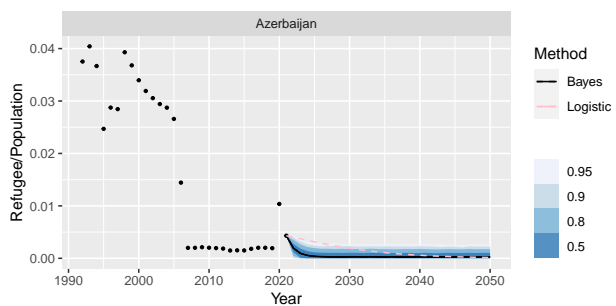
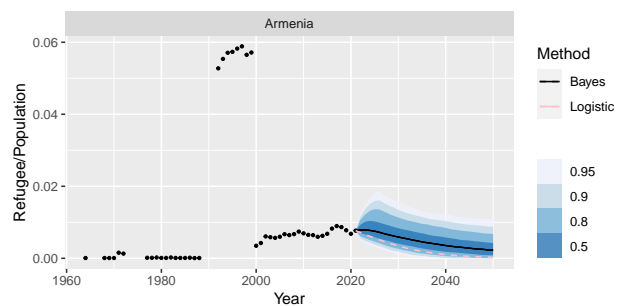
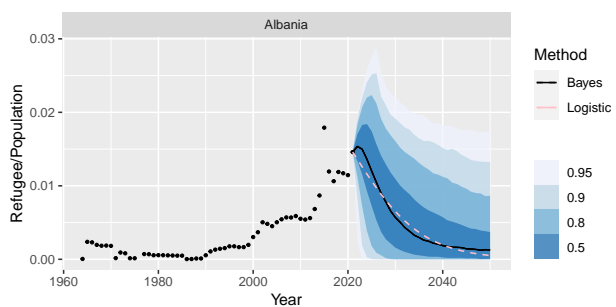
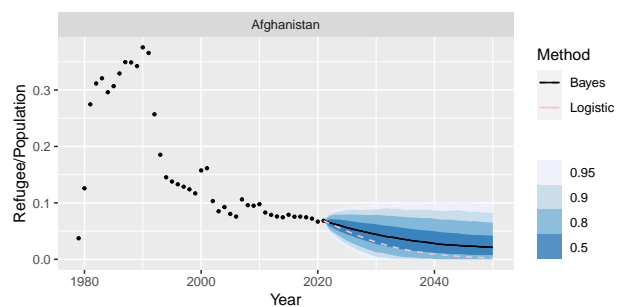
Growth and decline noise:

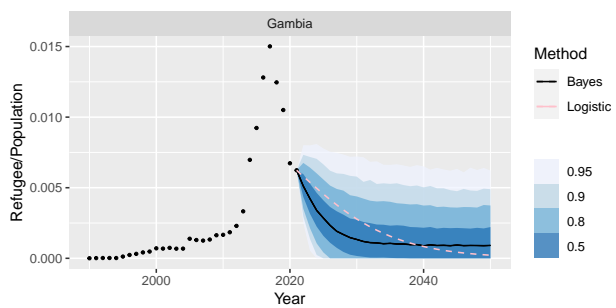
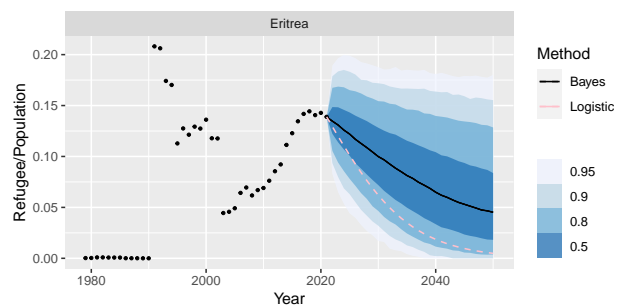
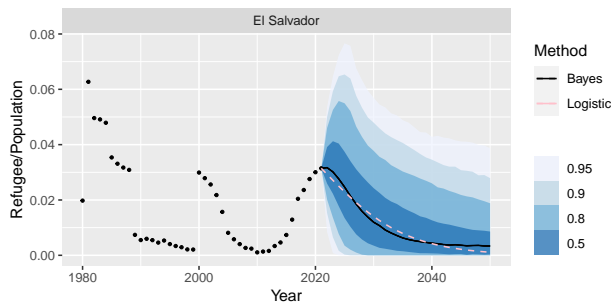
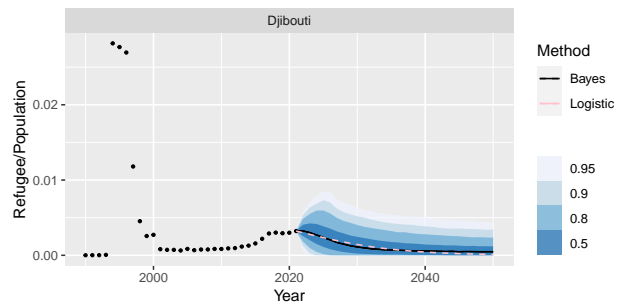
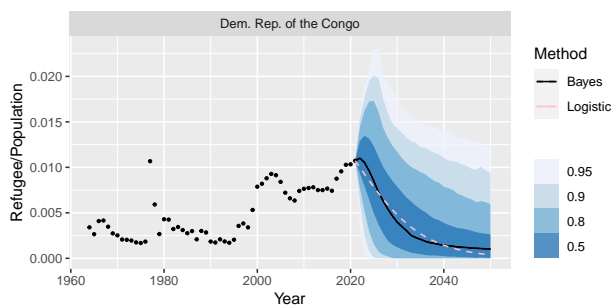
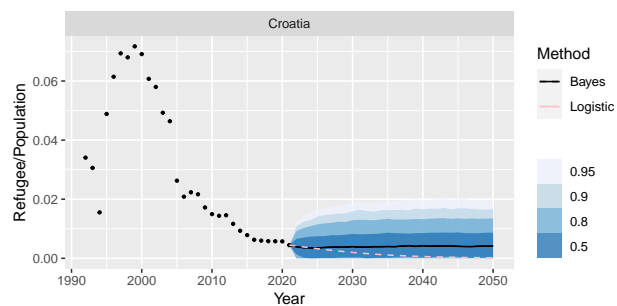
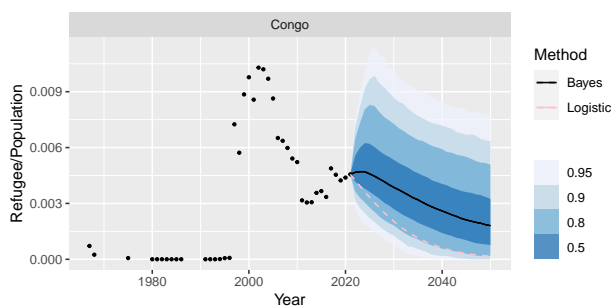
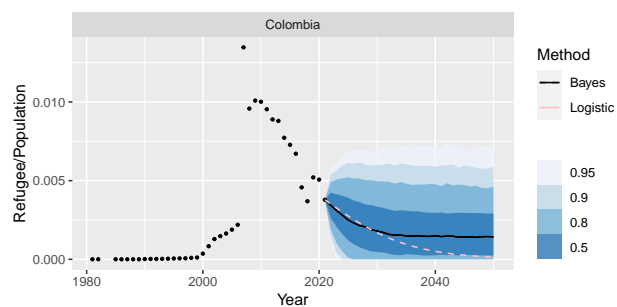
$$\begin{aligned}\mu_{\sigma^{(1)}} &\sim N(-7, 4), \\ \mu_{\sigma^{(2)}} &\sim N(-7, 4), \\ \sigma_{\sigma^{(1)}} &\sim \text{InvGamma}(0.1, 0.1) \\ \sigma_{\sigma^{(2)}} &\sim \text{InvGamma}(0.1, 0.1).\end{aligned}$$

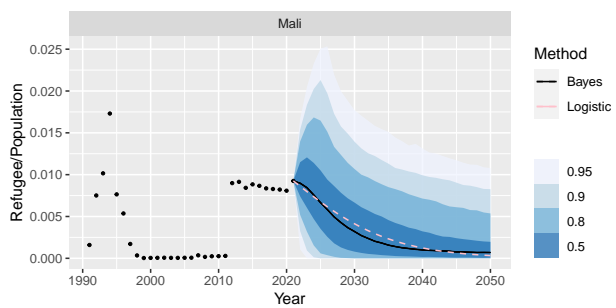
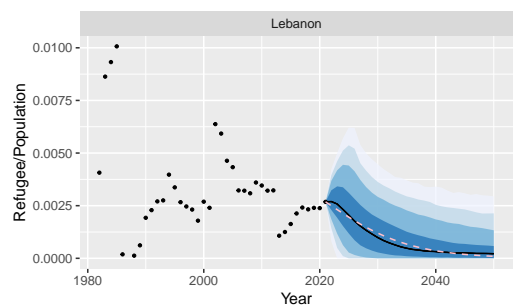
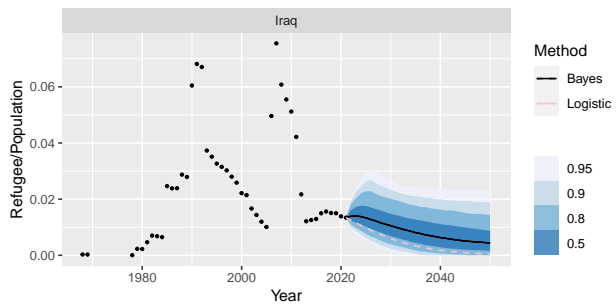
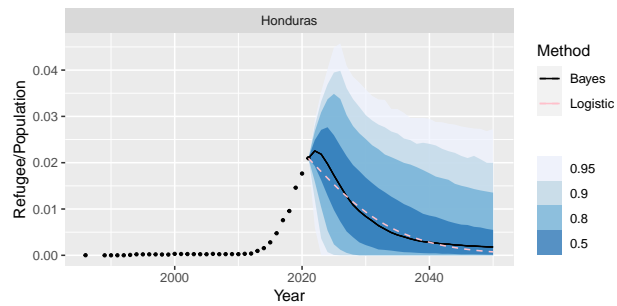
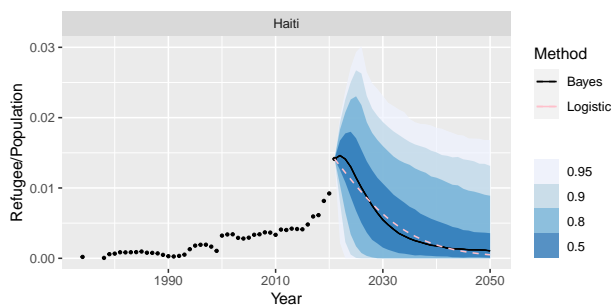
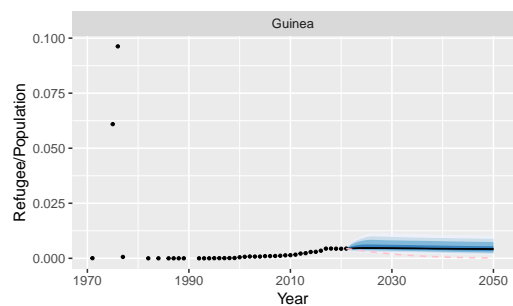
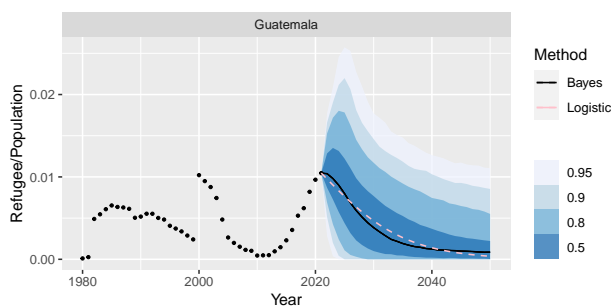
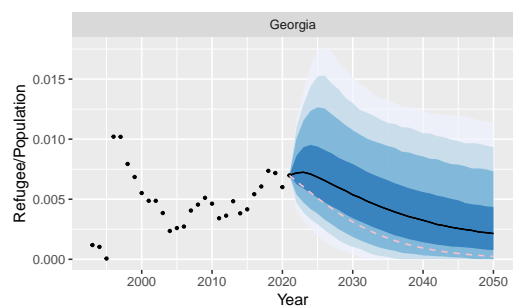
### Observed crisis lengths

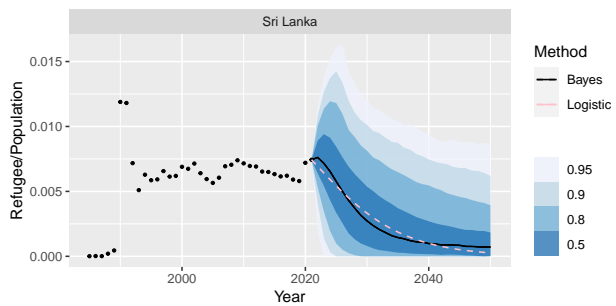
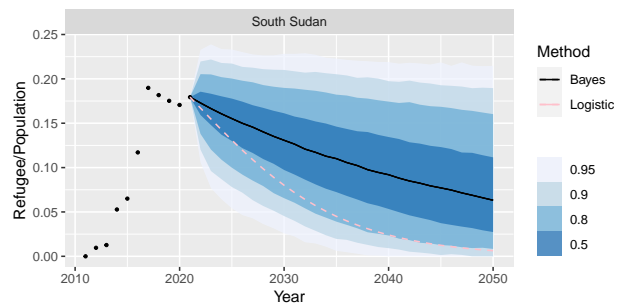
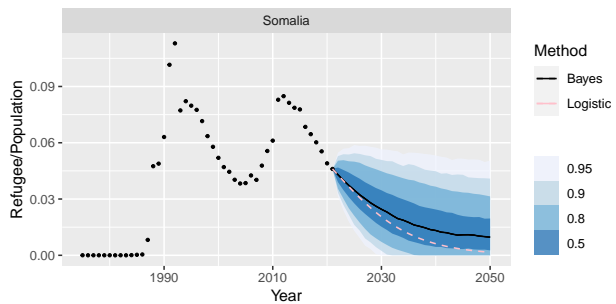
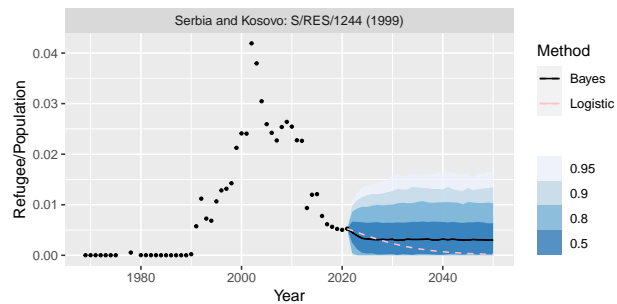
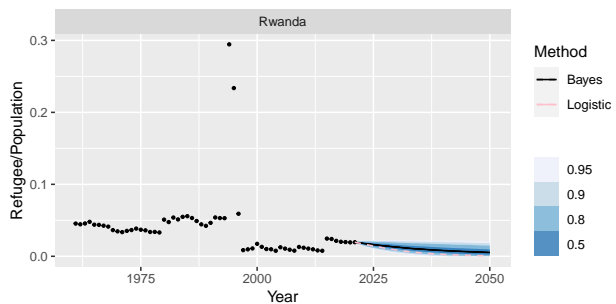
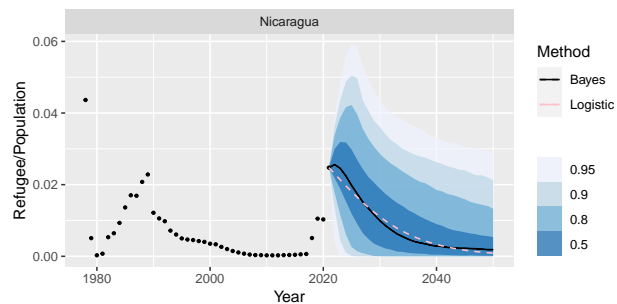
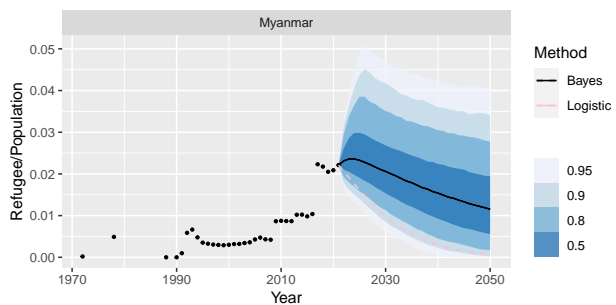
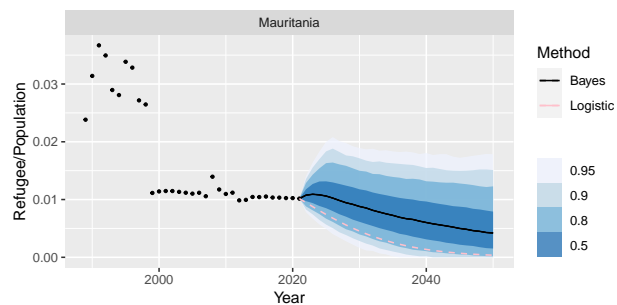
### Ongoing crisis predictions

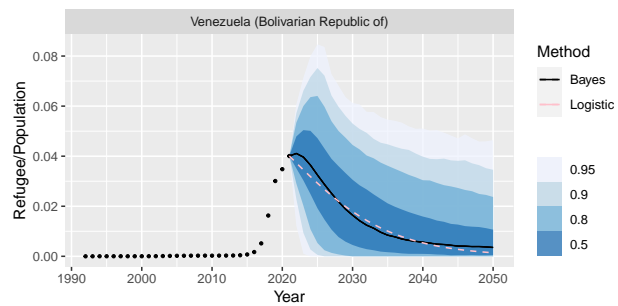
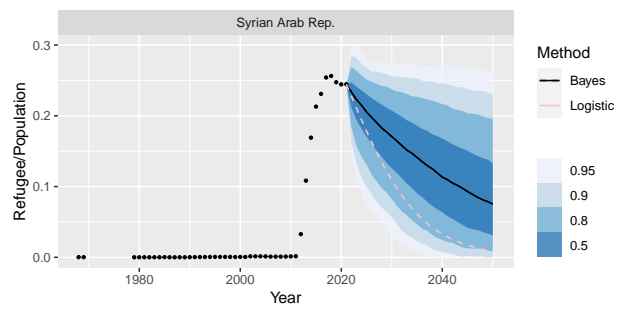
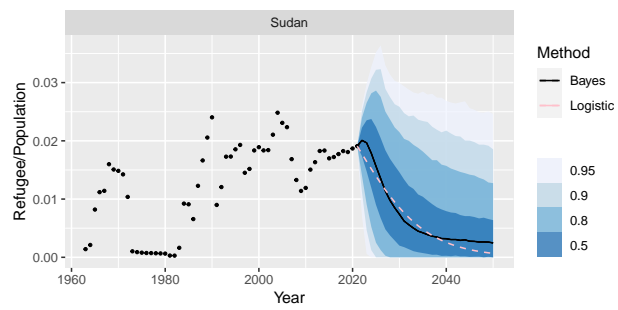
The plots below show the posterior predictive distributions for the refugee proportions  $\mu_{m,t}$  for all crises and time points. To simplify presentation, multiple crises from the same country are shown in the same plot.



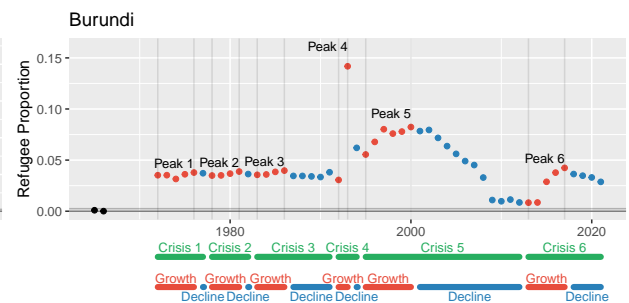
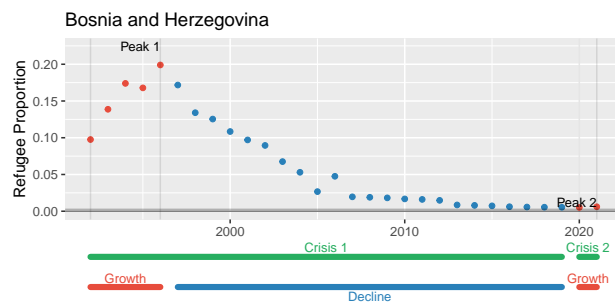
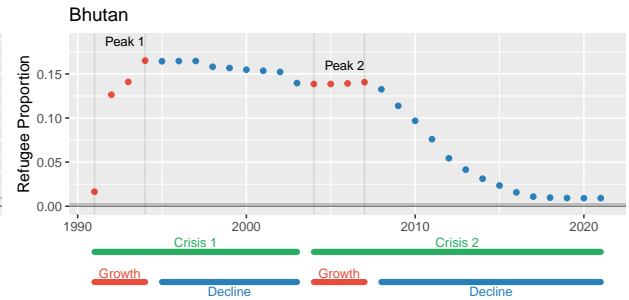
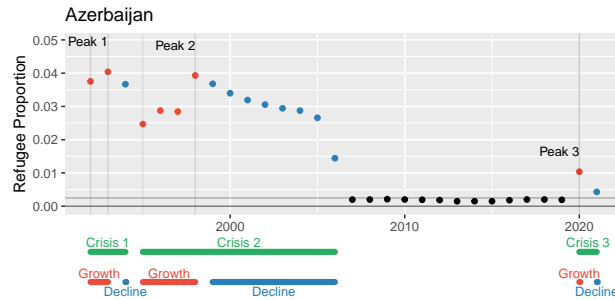
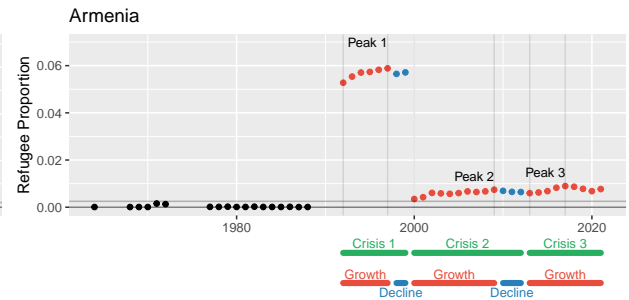
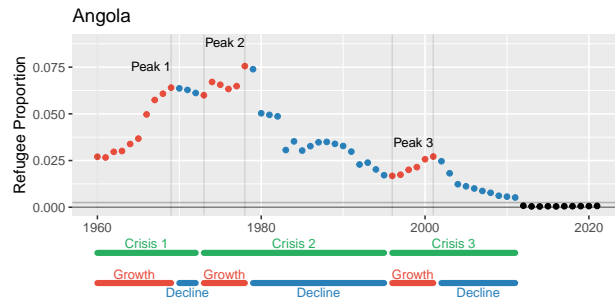
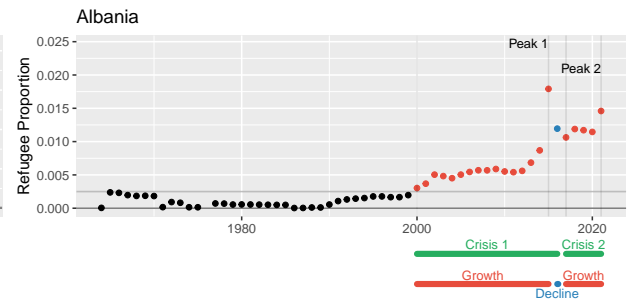
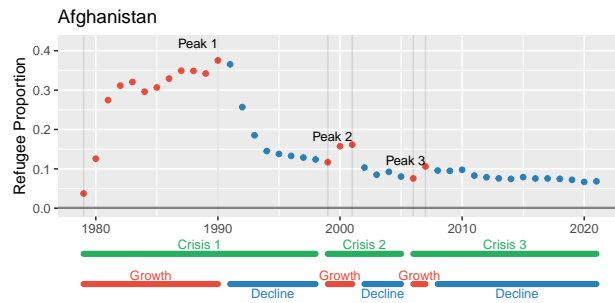




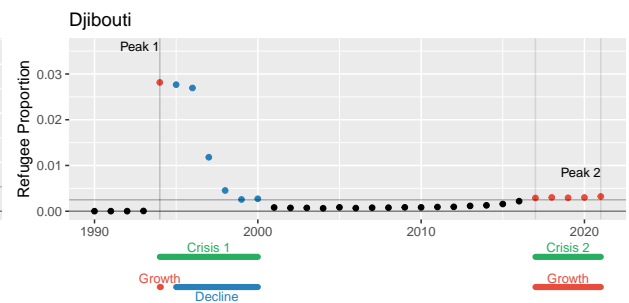
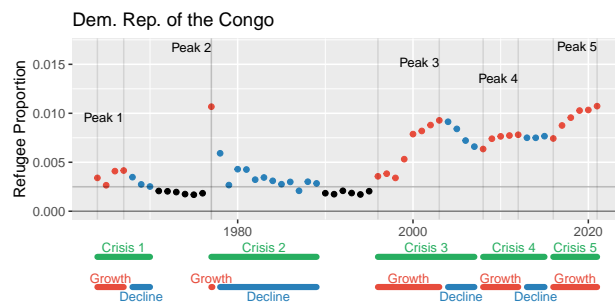
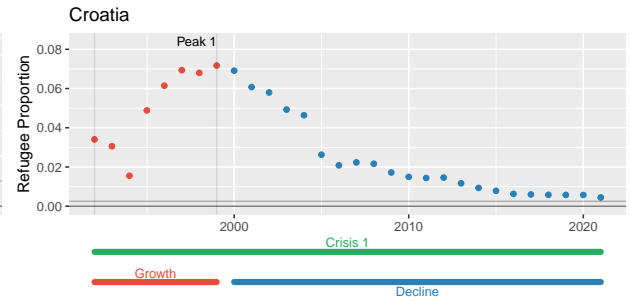
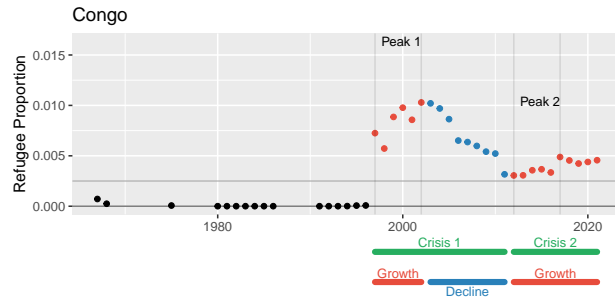
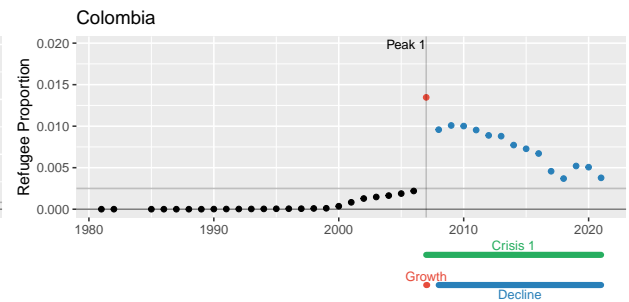
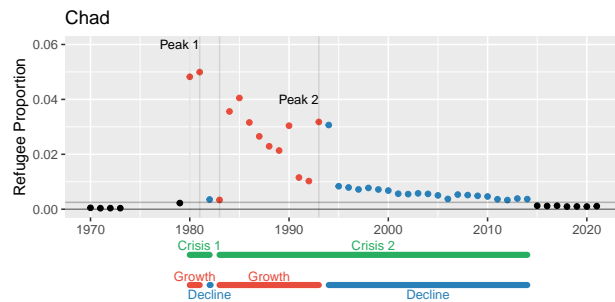
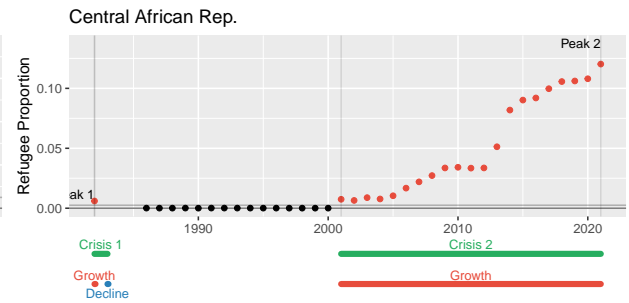
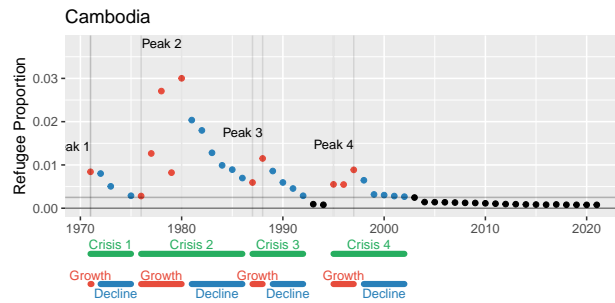


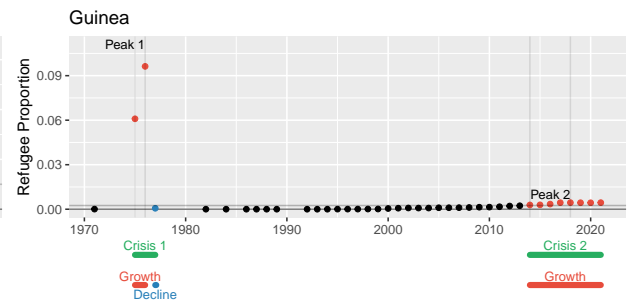
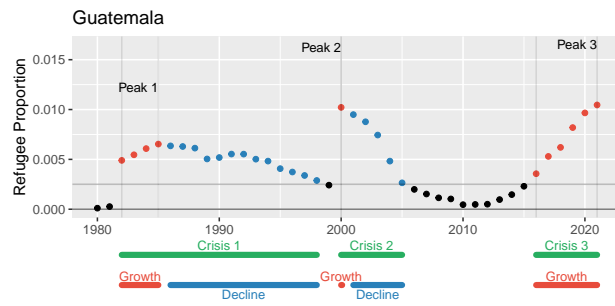
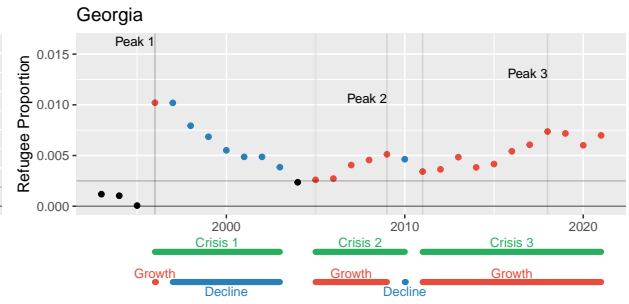
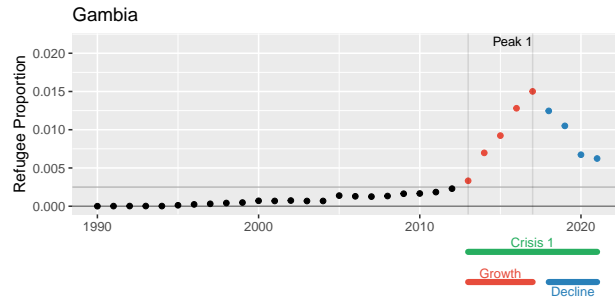
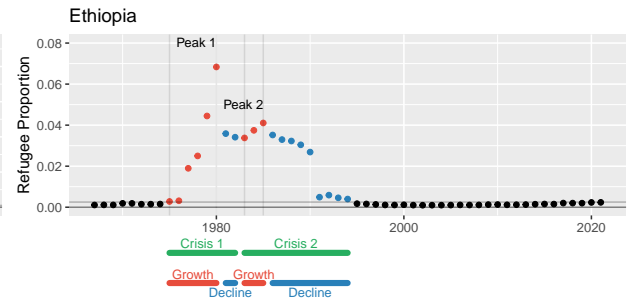
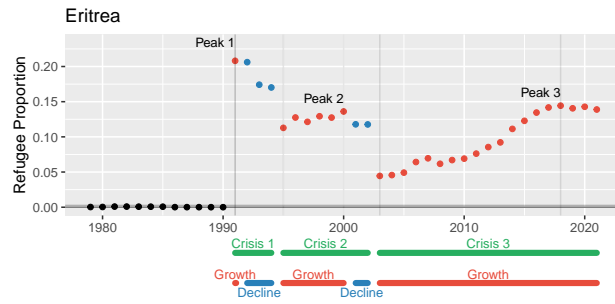
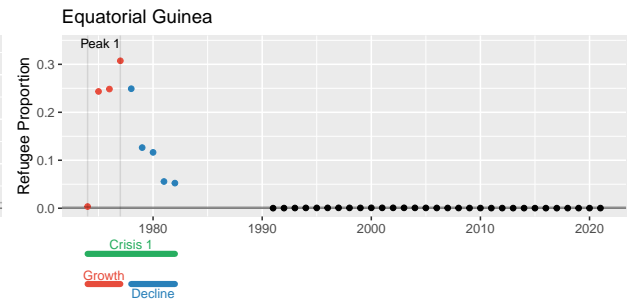
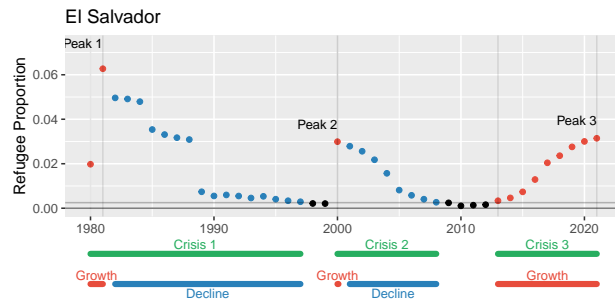


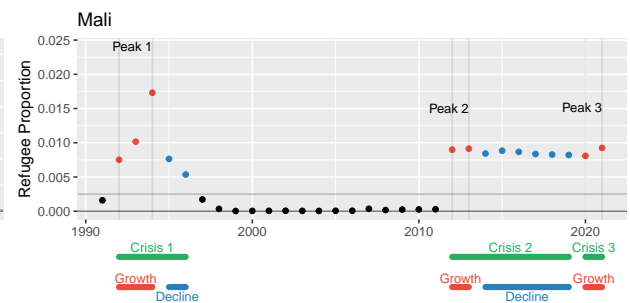
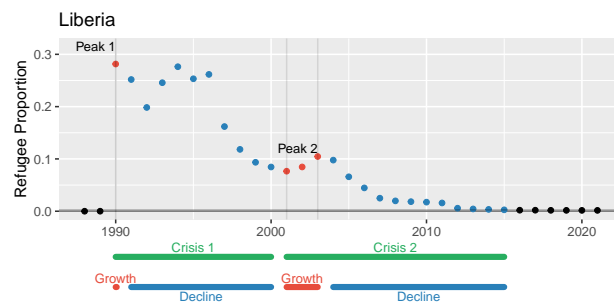
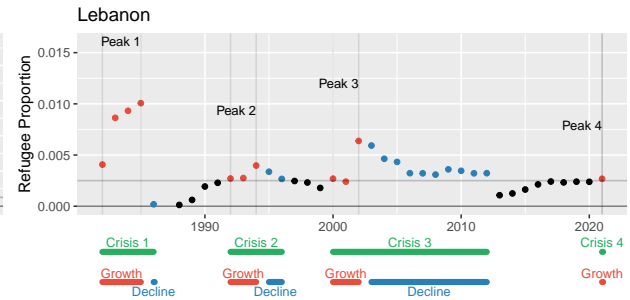
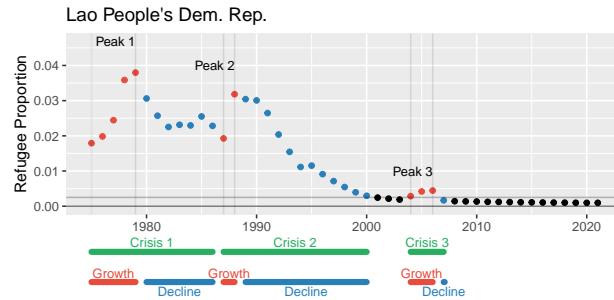
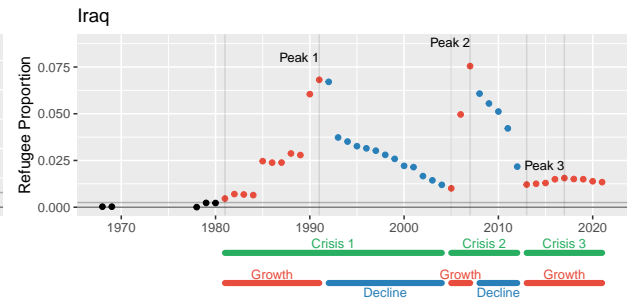
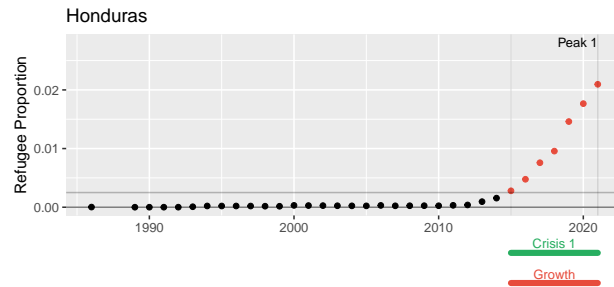
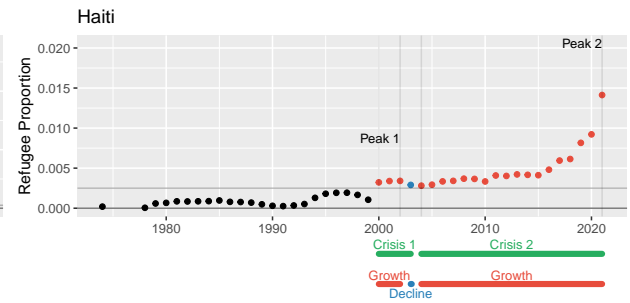
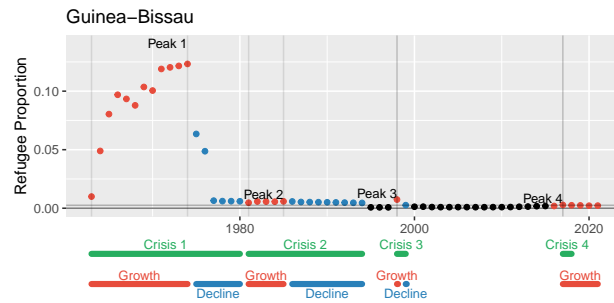
## 0.1 Crisis Segmentation

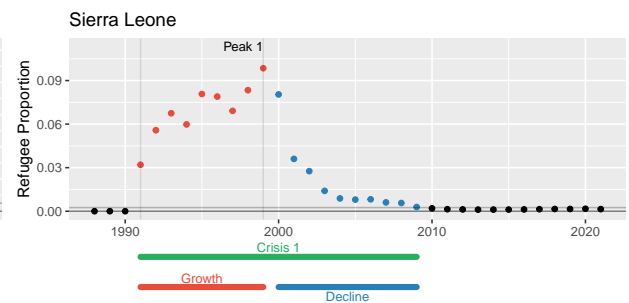
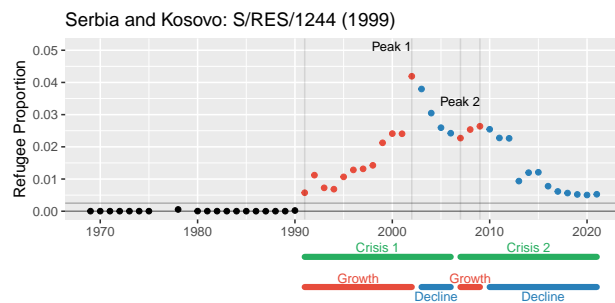
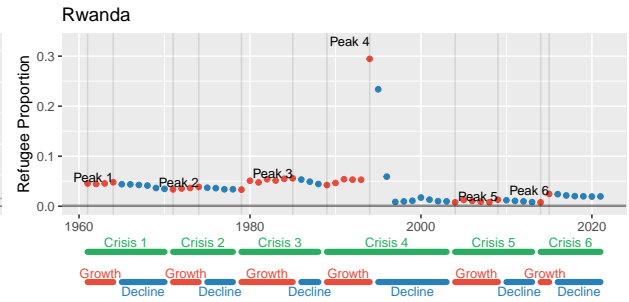
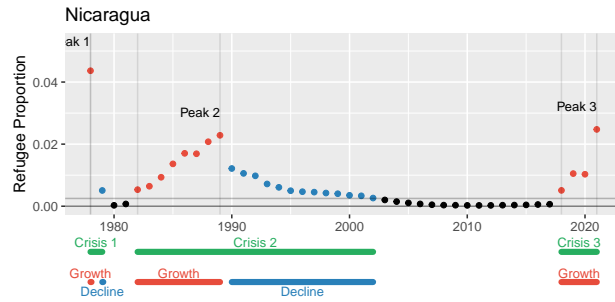
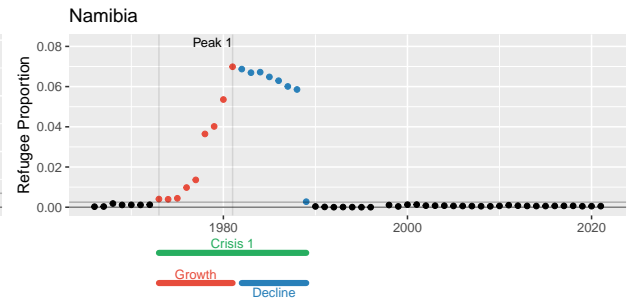
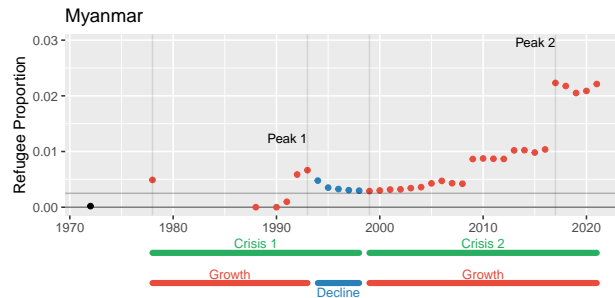
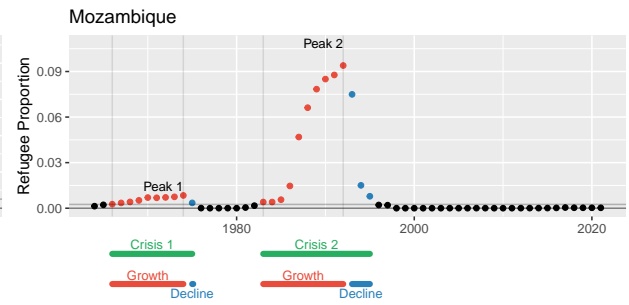
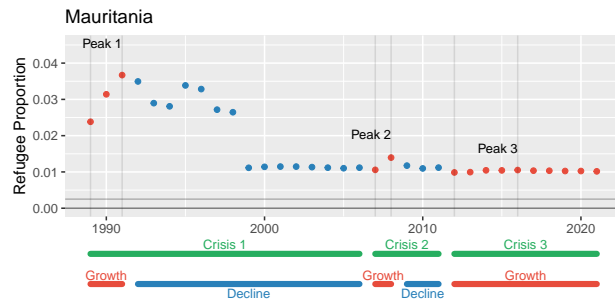


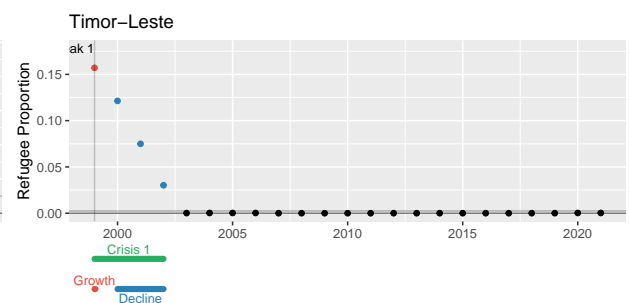
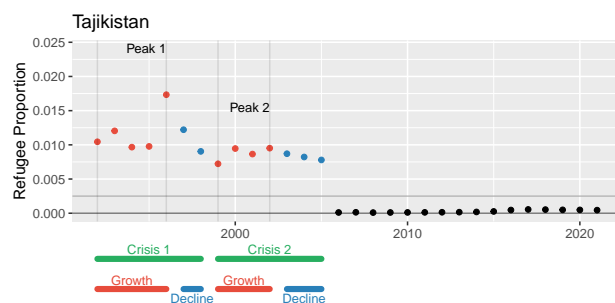
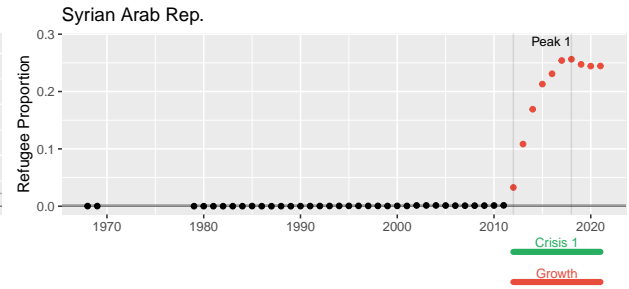
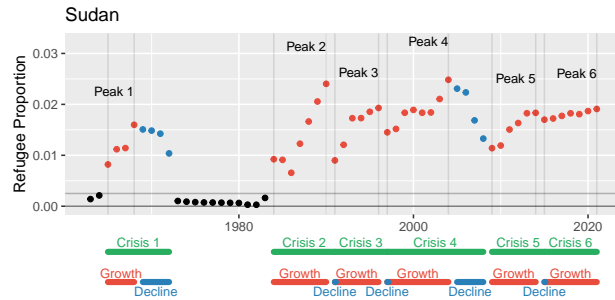
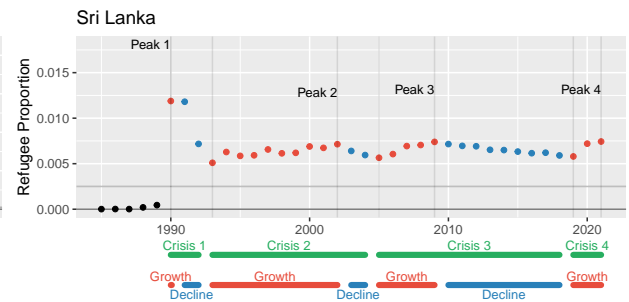
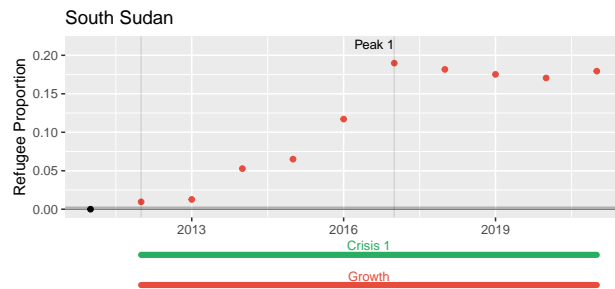
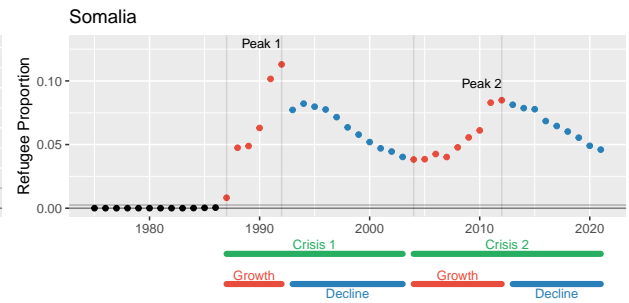
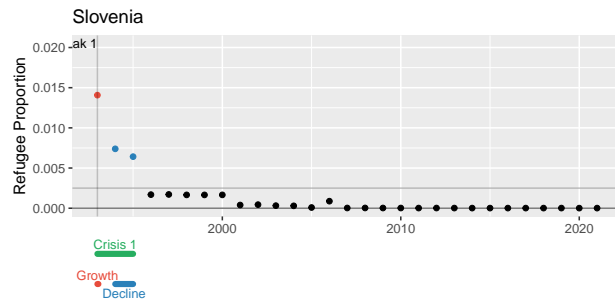


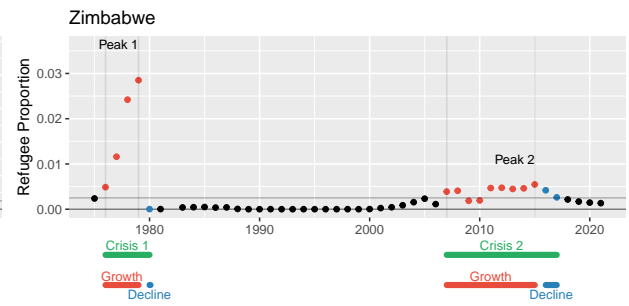
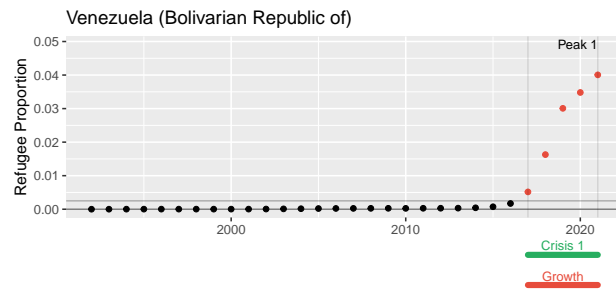
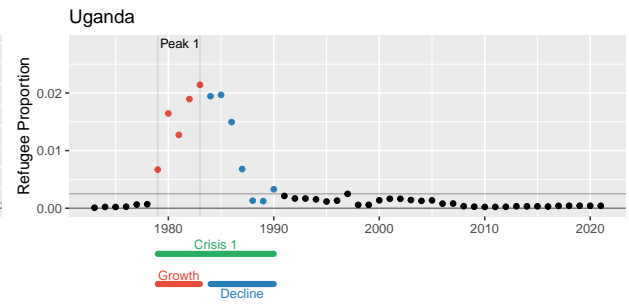
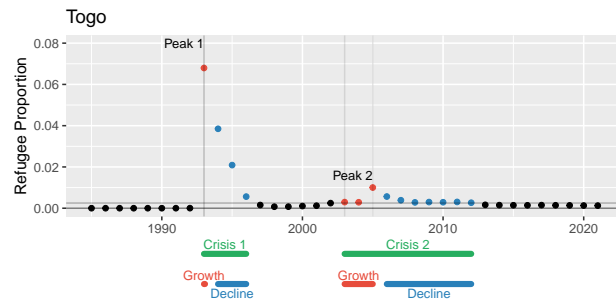












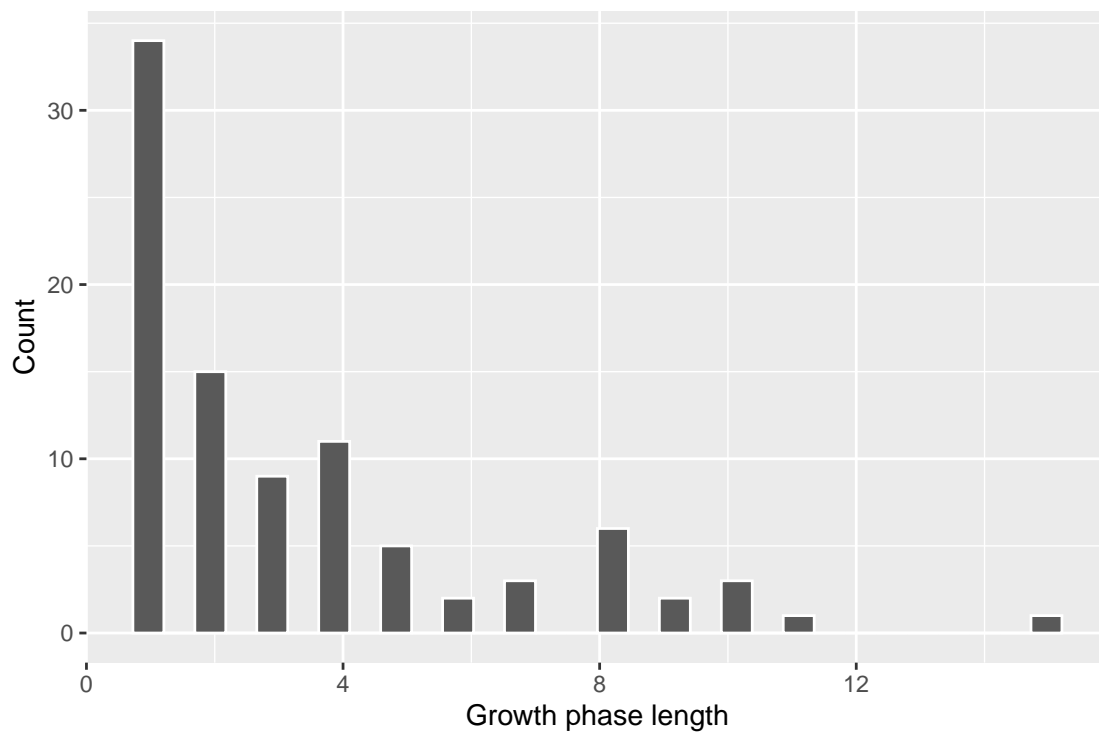


Figure 6: Empirical distribution of the length of the growth phase for all crises classified as ended.